Rare Metal Materials and Engineering
Volume 50, Issue 2, February 2021
Available online at www.rmme.ac.cn

Science Press

Cite this article as: Rare Metal Materials and Engineering, 2021, 50(2): 0469-0474.

ARTICLE

Non-contact Detecting Impact Damage Location for Composite Plate Based on HHT

Wang Ziping, Fei Yue, Qian Lei, Sun Si

Faculty of Civil Engineering and Mechanics, Jiangsu University, Zhenjiang 212013, China

Abstract: When aircraft, spacecraft, automobile, ship, or other engineering facilities are impacted by other objects during service, the damage may cause failure of the components or even catastrophic accidents. It is essential to take effective measures to monitor and assess such active impact damage. To locate impact damage precisely in real-time in an engineering structure, a non-contact impact damage location method based on scanning laser Doppler vibrometer (SLDV) was proposed. The Hilbert-Huang transform (HHT) was applied to the signal processing to obtain the best response frequency spectrum. The separated intrinsic mode function (IMF1) was used in the circular trajectory positioning imaging of amplitude total addition and amplitude multiplication. The experimental results indicate that HHT can be used to achieve non-contact impact damage location of composite materials.

Key words: impact damage; HHT; non-contact; SLDV; circular track positioning

Construction machinery structures, such as railways, bridges, airplanes, automobiles, and pressure vessels, will gradually accumulate damage due to corrosion, aging, and material fatigue, eventually leading to major accidents. For metal materials, the forms of damage include generation and extension of cracks and plastic deformation while for composite materials, the damage forms mainly include matrix cracking, delamination, and fiber breakage, etc.[1]. These defects will seriously affect their reliability, function, and durability[2]. Using structural health monitoring technology[3], the structure can be monitored in real-time, and the location and extent of damage can be quickly detected to prevent the occurrence of major accidents.

The Hilbert-Huang transform (HHT) is an advanced algorithm for non-linear, non-stationary signal processing[4]. It is based on an adaptive basis function, and its frequency is given by difference instead of convolution. The feature extraction is represented by time-frequency-energy space. HHT does not need a priori function, is adaptive[5], and can be used in processing abrupt signals, such as seismic signals, collision signals. Combined with the principle of random fuzzy statistics, the Hilbert marginal spectrum energy index is used to identify the damage in a beam bridge model[6]. In machining, HHT is used to analyze the vibration signal of the milling process, and it reflects the occurrence of vibration well and reveals the impact of each cutting edge on vibration[7]. According to the instantaneous energy variation established by HHT, the damage of a wing box structure can be judged[8]. In addition, research on response analysis and damage identification of seismic signals and composite structure signals based on the HHT method[9-11] is also in progress. The existing methods mostly use contact sensors to receive impact signals, which is inconvenient in engineering practice. Therefore, a non-contact signal acquisition method based on scanning laser Doppler vibrometer (SLDV) was proposed in this research. HHT[12-14] has been applied to analyze acoustic emission (AE) signal, which provides theoretical guidance in this research.

The characteristic frequency of a new damage was constructed based on HHT theory in this research. The intrinsic mode function (IMF1) decomposed by empirical mode decomposition (EMD) was applied to the damage

Received date: February 25, 2020
Foundation item: National Natural Science Foundation of China (11872191, 11520101001); Postgraduate Research & Practice Innovation Program of Jiangsu Province (KYCX19_1578)
Corresponding author: Wang Ziping, Ph. D., Associate Professor, Faculty of Civil Engineering and Mechanics, Jiangsu University, Zhenjiang 212013, P. R. China, E-mail: wzpxx2004@126.com

location, and the circular trajectory positioning method was applied to the impact location verification. The research results show that HHT can be used for the analysis and processing of impact signals, and can effectively locate impact damage by non-contact detection.

1 Basic Theory of Signal Processing and Damage Location

1.1 Hilbert-Huang transform

HHT consists of two main parts, namely EMD and Hilbert Transform. First, use EMD decomposition to decompose the complex signal into several time series from high frequency to low frequency and obtain the IMF, and then perform the Hilbert transform on the decomposed IMF. The time-spectrum characteristics of the original signal are available.

1.1.1 Empirical mode decomposition (EMD)

The Hilbert transform requires the signal to satisfy the narrowband condition, so a complex signal must be decomposed into a series of narrowband signals by the EMD method. These narrowband signals are the IMF, which needs to satisfy the conditions. The zero crossings and the extreme points of the signal are equal or at most one difference over the course of the time. At any point, the mean upper and lower envelopes defined by the local maximum and the local minimum are zero, i.e. the signal is locally symmetric about the time axis. EMD is a key step in the Hilbert-Huang transformation. The main steps are as follows.

(1) Assuming that the original data sequence is $x(t)$, all the local maxima and minima of the data sequence are found and interpolated by the cubic spline function to obtain the upper and lower envelopes x_{max} and x_{min} of the original sequence, respectively. Subtracting the envelope mean from the original data sequence yields:

$$h_1=x(t)-(x_{max}+x_{min})/2 \quad (1)$$

(2) Taking h_1 as the new $x(t)$, repeat Step 1 until h_1 satisfies the two conditions of the IMF, where h_1 is the first-order intrinsic mode function.

(3) Define the residual signal r_1 as:

$$r_1= x(t)-h_1 \quad (2)$$

Repeating the above steps with r_1 as the new signal yields a series of IMF components. Until the signal meets the standard deviation condition, the IMF screening is stopped at this time. After the end of EMD, the original signal can be expressed as follows:

$$x(t)=\sum_{i=1}^{n} h_i + r \quad (3)$$

where h_i is the IMF component of each order, and r is the residual function, representing the average trend of the signal. If the separated intrinsic mode function and residual function are added together, the original signal can be obtained.

1.1.2 Hilbert transform

The Hilbert transform is performed for the signal $x(t)$ satisfying the narrowband condition:

$$y(t)=\frac{1}{\pi}P\int_{-\infty}^{+\infty}\frac{x(\tau)}{t-\pi}\mathrm{d}\tau \quad (4)$$

where P is the Cauchy value and we can get its parsing signal:

$$z(t)=x(t)+iy(t)=a(t)\mathrm{e}^{i\theta(t)} \quad (5)$$

$$a(t)=\sqrt{x^2(t)+y^2(t)} \quad (6)$$

$$\theta(t)=\arctan\left(\frac{y(t)}{x(t)}\right) \quad (7)$$

By deriving the phase $\theta(t)$, the instantaneous frequency can be obtained:

$$\omega(t)=\frac{\mathrm{d}\theta(t)}{\mathrm{d}t} \quad (8)$$

After performing the Hilbert transform on each order IMF of the $x(t)$ decomposition, the Hilbert spectrum can be obtained:

$$H(\omega,t)=\sum_{j=1}^{n} a_j(t)\mathrm{e}^{i\int\omega_j(t)\mathrm{d}t} \quad (9)$$

where $a_j(t)$ is the amplitude of the analytical signal of the j^{th} order modal function. The Hilbert spectrum describes the distribution of the amplitude, time and frequency of the signal. The marginal spectrum $h(\omega)$ can be obtained from the Hilbert spectrum:

$$h(\omega)=\int_0^T H(\omega,t)\mathrm{d}t \quad (10)$$

The square of the $h(\omega)$ amplitude is integrated over time to obtain the Hilbert energy spectrum $E(\omega)$:

$$E(\omega)=\int_0^T H(\omega,t)^2\mathrm{d}t \quad (11)$$

The marginal spectrum provides amplitude distribution related to time and frequency, and the Hilbert energy spectrum reflects the energy accumulation for different frequencies of the signal in the sampling interval.

1.1.3 Principle of impact damage location based on SLDV

Fiber-reinforced composite materials are widely used in aerospace, aviation, civil engineering, and other fields, which have the characteristics of high strength, high corrosion resistance, heat resistance, and structural design. Due to their wide application range, they are involved in many major projects and key structures and easily damaged by the external environment. Therefore, epoxy fiberglass fiberboard was selected as the research object, and the impact localization experiment was carried out.

In the impact positioning experiment, a point was selected as the simulated impact point. The tap signal was received by the SLDV at a specific point, and the “Pitch-catch” mode was adopted. As shown in Fig.1, sensors 1, 2, and 3 form a triangular array. The distance between acoustic emission source A and sensor 1 is r. θ is the angle between the straight path of the sound source propagating to sensor 1 and the x-axis. δ_1 is the distance difference from the source to sensor 1 and sensor 2 while δ_2 is the distance difference from the

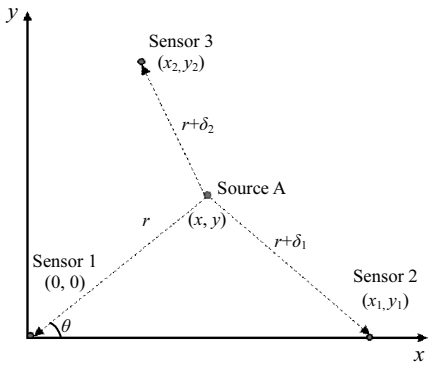

Fig.1 Positioning principle of three sensors for circle track

source to sensor 1 and sensor 3. Δt_{12} and Δt_{13} are the time differences of the signals arriving from source to sensors 1 and 2 and to sensor 1 and 3, respectively. v is the propagation speed of the acoustic emission signal. With sensors 1, 2, and 3 as the center of the circle, r, $r+\delta_1$, and $r+\delta_2$ are the radius, and three circles can be made. Sound source A is at the intersection of the three circles.

The distance difference can be expressed:

$$\delta_1=v\Delta t_{12},\ \delta_2=v\Delta t_{13} \tag{12}$$

It can be seen from the geometric relationship that

$$\begin{aligned} r &= \frac{A_1}{2(x_1\cos\theta + y_1\sin\theta + \delta_1)} \\ &= \frac{A_1}{2(x_2\cos\theta + y_2\sin\theta + \delta_2)} \end{aligned} \tag{13}$$

where

$$\begin{aligned} &A_1 = x_1^2 + y_1^2 - \delta_1^2 \\ &x_1\cos\theta + y_1\sin\theta + \delta_1 \neq 0 \\ &A_2 = x_2^2 + y_2^2 - \delta_2^2 \\ &x_2\cos\theta + y_2\sin\theta + \delta_2 \neq 0 \end{aligned} \tag{14}$$

Simplify Eq.(13):

$$\theta = \arctan\frac{A_1y_2 - A_2y_1}{A_1x_2 - A_2x_1} \pm \arccos\left|\frac{A_2\delta_1 - A_1\delta_2}{B}\right| + 2m\pi \tag{15}$$

(m=0, 1, 2…)

where

$$B = [(A_1x_2 - A_2x_1)^2 + (A_1y_2 - A_2y_1)^2]^{\frac{1}{2}} \tag{16}$$

SLDV was used to receive signals and eight receiving points was selected, three of which can be combined to achieve multiple components.

(1) Amplitude total addition. The signals with impact damage information obtained from multiple sets of points are added to the amplitude $B_i(t_i(x, y))$ of each point (x, y) in the plate. The imaging results are as follows:

$$B(x,y) = \sum_{i=1}^{N} B_i(t_i(x,y)) \tag{17}$$

(2) Amplitude multiplication. Multiply the amplitude $B_i(t_i(x, y))$ of each point (x, y) in the plate. The imaging results are as follows:

$$B(x,y) = \prod_{i=1}^{N} B_i(t_i(x,y)) \tag{18}$$

In Eq.(17) and Eq.(18), i represent the serial number of the corresponding sensor in the cell; x and y represent the coordinates of each point in the whole imaging region; $t_{ij}(x, y)$ refers to the time when the wave arrives at the sensor from a cell (x, y) in the plate. In short, the amplitude of the signal energy corresponding to each coordinate in the imaging region is calculated as "+" and "×" to enhance the final imaging effect.

2 Impact Positioning Experiment

2.1 Experimental preparation

The experimental instrument was a PSV-500 laser Doppler vibrometer. The experimental object was a 1000 mm×1230 mm×10 mm glass fiber epoxy resin composite plate placed vertically. As shown in Fig.2, the experimental platform built for the research consists of a PSV-500 scanning vibrometer, a power amplifier, and a fiberglass epoxy board. The composite plate is a glass fiber reinforced epoxy single-layer laminate with a 45° layup. As shown in Fig.2, the impact signal is collected on the composite panel using SLDV. On the surface of the board, 8 points (1~8) for collecting signals and point B for performing impact signal simulation are marked, and reflective paper is attached at the signal collection point. A piezoelectric piece is attached to point B, the impulse signal is simulated by the piezoelectric sheet excitation signal, and the signal is collected using the SLDV.

2.2 HHT signal analysis

The piezoelectric chip excitation signal was used to simulate the impact signal. As shown in Fig.3, the excitation signal is a five-peak wave with a central frequency of 150 kHz, the sampling point is 1024, and the signal is received at the specified point by SLDV. In this research, the five-peak wave signal is selected mainly because it has a certain bandwidth. As the excitation signal, the energy of the received signal is mainly concentrated in a frequency range. HHT transform can

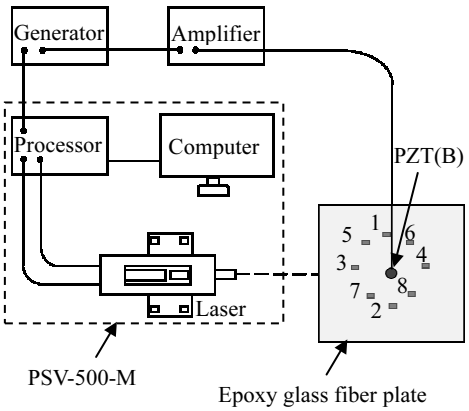

Fig.2 Impact positioning experimental platform

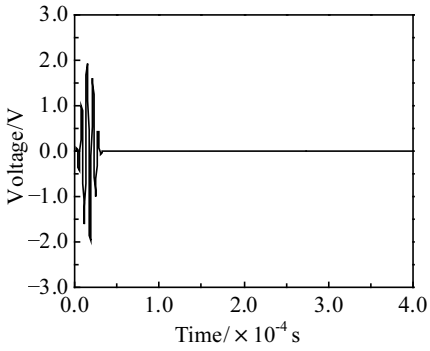

Fig.3 Excitation signal

separate the signals in each frequency band, so the required energy-concentrated frequency band can be extracted for imaging.

Fig.4 shows the EMD decomposition of a typical signal at one point received by SLDV. The EMD decomposition divides the original signal from high frequency to low frequency into 8 IMFs and a trend term residue (Res). Fig.5 shows the IMF decomposition for the original signal. Fig.5a~5e are the selected first-order to fifth-order IMF, respectively, and Fig.5f is Res. The waveform of IMF1 is close to the original signal, and its amplitude is the largest. As the decomposition progresses, its wavelength becomes longer and longer, the frequency becomes smaller and smaller, and its amplitude is large at the high-frequency part. As shown in Fig.5a, IMF1 has the largest amplitude and the highest frequency. The waveform is closer to the original signal at the effective frequency. The original signal is a multi-frequency signal, which can be used for impact location to achieve imaging in the time domain. However, the low-frequency part of the original signal will cause the size of the imaging region to be slightly larger than the filtered result. Moreover, for the five-peak wave signal with a central frequency of 150 kHz used for driving, the frequency band of the obtained signal itself is not very wide, and is mostly concentrated in the high-frequency part. Therefore, IMF1 can retain the high-frequency signal that provides the main contribution, so as to make the final imaging result more accurate. The residue (Res) is not a constant, but a curve, which reflects the trend of its change. In this research, IMF1 was selected as the signal of the final impact location, which is equivalent to remove all other low-frequency components and realize the signal filtering.

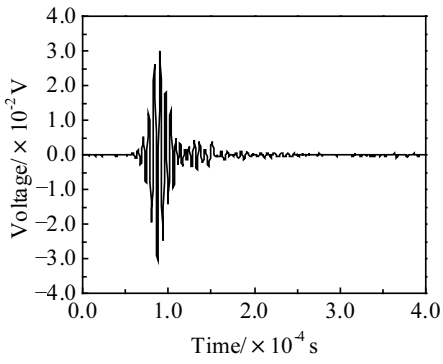

Fig.4 Original waveform

Fig.6 shows the 3D-HHT time-spectrum of the received signal. The time-frequency spectrum clearly describes the dynamic changes in energy over time and frequency. From this spectrum, we can get the amplitude corresponding to a certain frequency at a certain time. In Fig.5, the maximum peak frequency corresponds to 156 kHz, and the corresponding time is 8.8×10^{-5} s. Most of the energy is concentrated around 150 kHz, so the high-frequency component information can be effectively extracted by removing the low-frequency component by IMF1.

3 Impact Location Experiment Results

The glass fiber reinforced epoxy resin board can be approximated as an isotropic material. Therefore, sound velocity calibration was performed in three directions, namely 0°, 45°, and 90°. Multiple groups of data were selected for averaging, and the wave packet velocity was obtained, which was 2399 m/s.

The imaging method adopted in this research is based on the three-sensor circular trajectory positioning method. Since there are 8 measuring points, 8 circles are used for the intersection. First, the imaging area is meshed. According to the distance from the point in the imaging area to the receiving point, by comparing with the speed, the time matrix of the wave reaching each point can be obtained, and then the time is compared with the sampling time interval. Find the corresponding amplitude from the corresponding signal, and then fill it into each cell to get a single receiving point image. Eight graphs can be fused by amplitude multiplication and full data fusion methods to obtain the final imaging results.

The final imaging results are shown in Fig.7 and Fig.8, where the white circle is the actual position of the piezoelectric sheet and its coordinate of center position is (180 mm, 240 mm). Fig.7 is the comparison between actual position and imaging result of amplitude total addition method. Fig.7 shows that the coordinate of the highest point of the pixel in the deep red region is (186 mm, 239 mm), the error in the center position of the piezoelectric sheet is 6.08 mm, and the piezoelectric sheet is basically positioned. Fig.8 indicates the imaging results of IMF1 using amplitude multiplication method. The dark red range is small, and it is basically covered by the piezoelectric sheet. The coordinate with the highest amplitude is 184 mm, 238 mm, the error in the center position of the piezoelectric sheet is 4.47 mm. It is already in the size range of the piezoelectric plate. Table 1 is the summary of the final

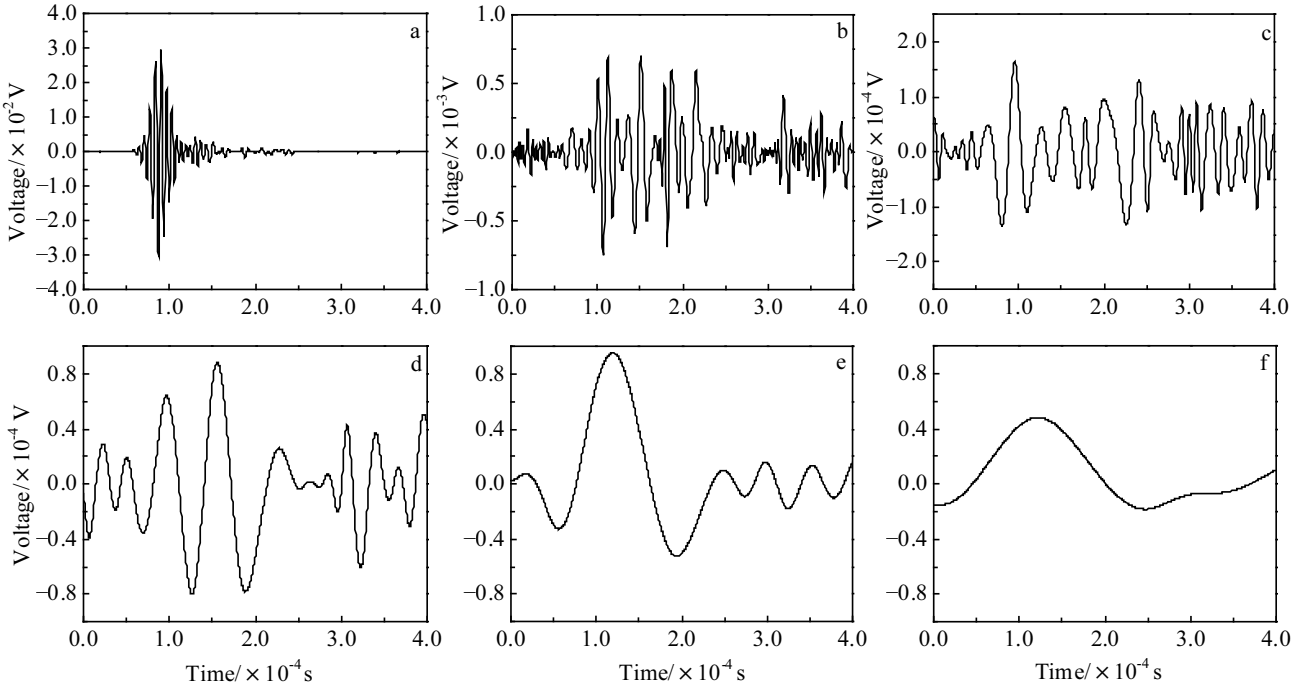

Fig.5 Empirical mode decomposition IMF results: (a) IMF 1, (b) IMF 2, (c) IMF 3, (d) IMF 4, (e) IMF 5, and (f) Res

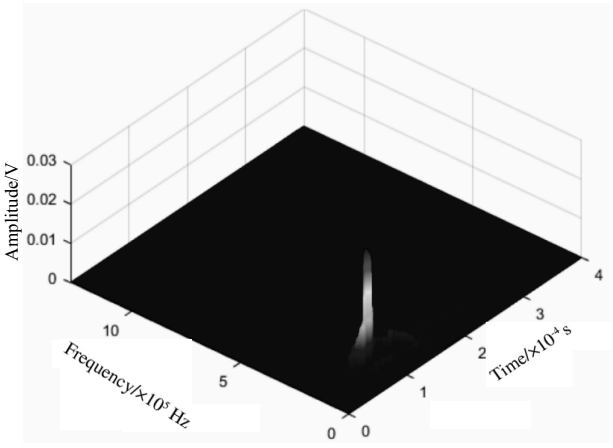

Fig.6 3D time spectrum of the received signal

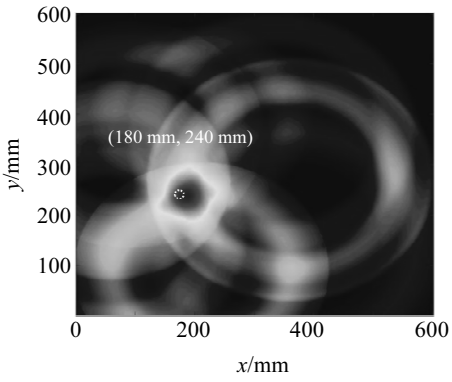

Fig.7 Imaging results of amplitude total addition method

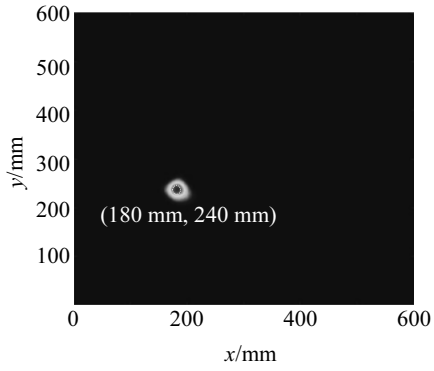

Fig.8 Imaging results of amplitude multiplication method

results. The error of the two methods is within the controllable range, and for the amplitude total addition and amplitude multiplication data fusion algorithms, the amplitude multiplication is better since the positioning range is smaller and the precision is higher. By comparing the results of the original signal and IMF1, it can be seen that the accuracy of IMF1 is higher than that of the original signal. Since the HHT method is an empirical method, the separated modes still have overlapping portions, which results in a slight deviation in the results.

Table 1 Summary of imaging results

Method	Actual coordinate/mm	Resulting coordinate/mm	Error/mm
Amplitude total addition (original waveform)	(180, 240)	(188, 240)	8
Amplitude multiplication (original waveform)	(180, 240)	(188, 236)	8.94
Amplitude total addition (IMF1)	(180, 240)	(186, 239)	6.08
Amplitude multiplication (IMF1)	(180, 240)	(184, 238)	4.47

4 Conclusions

1) SLDV can be used to collect shock signals and has non-contact characteristics, avoiding traditional contact and bringing convenience to practical applications.

2) The EMD method can effectively and adaptively decompose the complex signal into IMF sequences of different time scales and can obtain the required frequency band by screening and removing the unnecessary bands.

3) The HHT method can express the time-frequency characteristics of the signal through the marginal spectrum, Hilbert spectrum, etc., and obtain the optimal response frequency to complement the nonlinear and non-stationary signal time-frequency analysis.

4) The first-order IMF obtained by the decomposition is the characteristic mode, and the obtained imaging result has a small error with the actual impact position, which verifies the feasibility of this method.

5) Using the amplitude total addition and amplitude multiplication method for impact location imaging based on the circular trajectory method, the simulated impact damage location can be accurately located.

References

1 Girolamo Donato, Chang Huan-Yu, Yuan Fuh-Gwo. *Ultrasonics*[J], 2018, 87: 152

2 Wang Z, Luo Y, Zhao G *et al*. *Research in Nondestructive Evaluation*[J], 2016, 27(4): 204

3 Sang S. *Acta Mechanica*[J], 2018, 229(6): 2561

4 Trung N T. *Structural Control and Health Monitoring*[J], 2019, 26(10): 2427

5 Victoria G S M, Maximiliano B L, Marta M *et al*. *IEEE Latin America Transactions*[J], 2018, 16(4): 1091

6 Gu Aijun, Luo Ying, Xu Baiqiang. *Structural Health Monitoring*[J], 2016, 15(1): 104

7 Susanto A, Liu C H, Yamada K *et al*. *Precision Engineering*[J], 2018, 53: 263

8 Chen H G, Yan Y J, Jiang J S. *Mechanical System & Signal Processing*[J], 2007, 21(1): 307

9 Ding G, Xiu C, Wan Z *et al*. *Molecules*[J], 2019, 24(19): 3524

10 Shang H, Wang Y. *Sixth International Symposium on Instrumentation and Control Technology: Sensors, Automatic Measurement, Control, and Computer Simulation*[C]. Bellingham: International Society for Optics and Photonics, 2006, 6358: 635 801

11 Wang T, Zhang M, Yu Q *et al*. *Journal of Applied Geophysics*[J], 2012, 83: 29

12 Huang N E. *Hilbert-Huang Transform and Its Applications*[M]. Singapore: World Scientific Press, 2014

13 Wang Ziping, Luo Ying, Zhao Guoqi *et al*. *International Journal of Mechanics and Materials in Design*[J], 2017, 13(1): 57

14 Liu Z, Chen H, Sun K *et al*. *Journal of Visualization*[J], 2018, 21(5): 751

基于 HHT 的复合板非接触冲击损伤定位研究

王自平，费 跃，钱 磊，孙 思

(江苏大学 土木工程与力学学院，江苏 镇江 212013)

摘 要：航空/航天器、汽车、轮船等工程设施在服役过程中受到其他物体的冲击时，造成的损伤会引起构件的失效甚至会造成灾难性事故，如何采取有效的措施监测和评定这类活性冲击损伤至关重要。为了实现实时、准确地定位工程结构中的冲击损伤，提出了一种基于扫描式激光多普勒测振仪（SLDV）的非接触式冲击损伤定位方法。将希尔伯特黄变换（Hilbert-Huang transform, HHT）应用于信号处理中，得出最佳响应频率谱，将分离出的本征模函数（IMF1）用于幅值全加和幅值全乘的圆轨迹定位成像中。实验结果表明，HHT 方法可用于实现复合材料的非接触式冲击损伤定位中。

关键词：冲击损伤；希尔伯特黄变换；非接触；激光多普勒测振；圆轨迹

作者简介：王自平，男，1979 年生，博士，副教授，江苏大学土木工程与力学学院，江苏 镇江 212013，E-mail: wzpxx2004@126.com